

Formation rates of core collapse SNe and GRBs

Robert G. Izzard, Enrico Ramirez-Ruiz and Christopher A. Tout

Institute of Astronomy, Madingley Road, Cambridge, CB3 0HA

16 September 2018

ABSTRACT

Core collapse of massive stars with a relativistic jet expulsion along the rotation axis is a widely discussed scenario for gamma-ray burst (GRB) production. However the nature of the stellar progenitor remains unclear. We study the evolution of stars that may be the progenitors of long-soft GRBs – rotating naked helium stars presumed to have lost their envelopes to winds or companions. Our aim is to investigate the formation and development of single and binary systems and from this population evaluate the rates of interesting individual species. Using a rapid binary evolution algorithm, that enables us to model the most complex binary systems and to explore the effect of metallicity on GRB production, we draw the following conclusions. First we find that, if we include an approximate treatment of angular momentum transport by mass loss, the resulting spin rates for single stars become too low to form a centrifugally supported disc that can drive a GRB engine – although they do have sufficiently massive cores to form black holes. Second massive stars in binaries result in enough angular momentum – due to spin-orbit tidal interactions – to form a centrifugally supported disc and are thus capable of supplying a sufficient number of progenitors. This holds true even if only a small fraction of bursts are visible to a given observer and the GRB rate is several hundred times larger than the observed rate. Third low-metallicity stars aid the formation of a rapidly rotating, massive helium cores at collapse and so their evolution is likely to be affected by the local properties of the ISM. This effect could increase the GRB formation rate by a factor of 5–7 at $Z = Z_{\odot}/200$. Finally we quantify the effects of mass loss, common-envelope evolution and black-hole formation and show that more stringent constraints to many of these evolution parameters are needed in order to draw quantitative conclusions from population synthesis work.

Key words: gamma-rays: bursts – stars: supernovae – X-rays: sources

1 INTRODUCTION

Gamma-ray bursts (GRBs) are intense flashes of gamma-rays which, for a few seconds, light up an otherwise dark gamma-ray sky. They are detected about once a day and outshine every other gamma-ray source in the sky. Major advances have been made in the last few years including the discovery of slowly fading X-ray (Costa et al. 1997), optical (van Paradijs et al. 1997) and radio (Frail et al. 1999) afterglows of GRBs, the identification of host galaxies at cosmological distances and the evidence that many of them are associated with star forming regions and possibly supernovae (see Mészáros 2001 for a recent review). Given the twin requirements of enormous energy, about 10^{53} erg, and association with star forming regions, the currently favoured models all involve massive, collapsing stars and their end products, especially black holes.

Hyper-accreting black holes (0.01 to $10 M_{\odot} \text{ s}^{-1}$) can arise from collapsars of various types (Woosley 1993; Fryer et al. 2001); white dwarf-black hole mergers (Frail et al. 1999; Belczynski et al. 2002a); helium core-black hole mergers (Fryer & Woosley 1998; Belczynski et al. 2002a); and merging neutron stars and black holes (Kluźniak & Lee 1998; Ruffert & Janka 1999; Lee & Ramirez-Ruiz 2002). Those models that involve merging neutron stars and black holes mostly transpire outside star forming regions and are not currently thought to be appropriate for long GRBs (Mészáros 2001). Of the other accretion-based models, black holes merging with both helium cores and white dwarfs have the advantage that they could occur in star forming regions (Belczynski et al. 2002a), produce adequate energy, and have sufficient angular momentum to form a disc. However, if the burst is to be beamed to less than 1% of the sky, the white dwarf model may provide an inadequate number of events (Fryer et al. 1999). The helium core model requires that a hydrogen envelope initially be present in order that the black hole (or neutron star) experience a common envelope evolution and merge with the core. Yet the same envelope must be absent when the burst occurs or prohibitive baryon loading will occur (MacFadyen et al. 2001). It may be that the merger peels off the envelope as the compact remnant goes in, but calculations to support this hypothesis are needed. It should be noted that the merger of a black hole with a massive helium core produces essentially the same conditions as in ordinary collapsars, except for a larger angular momentum. The beaming and energetics should also be comparable.

A collapsar forms when the evolved core of a massive star collapses to a black hole, either by fallback or because the iron core fails to produce an outgoing shock (Woosley 1993; Paczyński 1998; MacFadyen & Woosley 1999). Prompt and delayed black hole formation may occur in stars with a range of radii depending on the evolutionary state of the massive progenitor, its metallicity

and its multiplicity. The two necessary ingredients for the collapsar are a failed or weak initial supernova (SN) explosion that produces a black hole and sufficient angular momentum to form a disc. Energy dissipated in the disc or the rotation of the black hole itself is assumed to power a jet of high Lorentz factor $\Gamma \approx 100$ (Soderberg & Ramirez-Ruiz 2002) which escapes the stellar progenitor along the polar axis.

The traversal time for the relativistic jet through the hydrogen envelope of a typical massive star ranges from hundreds to thousands of seconds. At the time of the burst naked helium stars, which have radii of only a few light seconds, are required if the lifetime of the engine is not to be short when compared with the time it takes the jet to tunnel through the star (MacFadyen & Woosley 1999; Aloy et al. 2000; Wheeler et al. 2000; Mészáros & Rees 2001; Mészáros & Waxman 2001; Ramirez-Ruiz, Celotti & Rees 2002; Matzner 2003). This is aided if the stellar progenitor undergoes a Wolf-Rayet (WR) phase characterised by a strong stellar wind that causes the star to lose enough of its outer layers for the surface hydrogen abundance to become minimal (MacFadyen & Woosley 1999; Ramirez-Ruiz et al. 2001). The radius of a WR star is then sufficiently small for the jet to emerge before the engine ceases to operate. Break-out is further helped if the progenitor originates in a low-metallicity environment, when stars are smaller in radius, lose less mass and consequently have more massive cores. Both effects are thought to favour GRB formation (MacFadyen & Woosley 1999; Fryer et al. 1999).

Here we present population synthesis calculations which allow us to explore what effect initial mass, metallicity and membership in a binary system have on GRB production. In addition to all aspects of single-star evolution, our rapid evolution algorithm includes features such as mass transfer, mass accretion, common-envelope evolution, collisions, SN kicks and angular-momentum-loss mechanisms which enables us to model even the most complex binary systems. The binary-evolution algorithm is described in detail in Section 2. Section 3 contains the results of binary and single populations of core collapse SNe in solar metallicity environments. We also quantify the effects that mass loss, common-envelope evolution, and black-hole formation have on GRB production. The various kinds of companion remnants that are expected when the primary massive star collapses to a black hole are also discussed in Section 3. We present the results of population synthesis to examine the effects of metallicity in Section 4 and compare our model results with observations in Section 5. Our conclusions are then given in section 6.

2 STELLAR EVOLUTION MODELS

2.1 A field guide to stellar evolution

A fundamental tool in stellar evolution is the Hertzsprung-Russell diagram (HRD) which provides a correspondence between the observable stellar properties – the effective surface temperature T_{eff} and luminosity L . Fig. 1 shows the evolution of a collection of stars in the HRD from the zero-age main sequence (ZAMS), where a star adjusts itself to nuclear and hydrostatic equilibrium, until the end of nuclear burning. As stars take a relatively short time to reach the ZAMS after molecular cloud collapse, all ages are measured from this point. The span of a star’s life, its path on the HRD and its ultimate fate depend critically on its mass.

The immediate post-MS evolution towards the right in the HRD occurs at nearly constant luminosity and is very rapid. For this reason very few stars are seen in this phase, and this region of the HRD is called the Hertzsprung gap (HG) or the sub-giant branch. During this HG phase the radius of the star increases greatly causing a decrease in T_{eff} . As the convective envelope grows in extent the star reaches the giant branch (GB). Eventually a point is reached on the GB where the core temperature is high enough for stars to ignite their central helium supply. When core helium burning (CHeB) begins the star descends along the GB until contraction moves the star away from the fully convective region of the HRD and back towards the MS in what is called a blue loop. During CHeB, carbon and oxygen are produced in the core. Eventually core helium is exhausted and the star moves back to the right in the HRD. Stars of very high mass ($M_{\text{zams}} > 25M_{\odot}$) reach high enough central temperatures on the HG for helium to ignite before reaching the GB.

Evolution after the exhaustion of core helium is very similar to that occurring after core-hydrogen exhaustion at the end of the MS – the convective envelope deepens again to begin what is called the asymptotic giant branch (AGB). On the AGB the star is now a dense core composed of carbon and oxygen surrounded by a helium burning shell which in turn adds carbon (and some oxygen) to the degenerate core. Initially the H-burning shell is weak so that the luminosity is supplied by the He-burning shell. During this phase, the stellar radius grows significantly.

The surface gravity of the star is lowered so the surface material is less tightly bound. Mass loss from the stellar surface becomes significant with the rate of mass loss increasing with time. Unfortunately our understanding of the mechanisms that cause this mass loss is poor with possible suggestions linking it to the helium shell flashes or to periodic envelope pulsations. Whatever the cause, the influence on the evolution of AGB stars is significant. Mass loss eventually removes all of the star’s envelope so that the H-burning shell shines through.

If the mass of the star is large enough, $M_{\text{zams}} \gtrsim 7M_{\odot}$ (although the exact value depends on its metallicity and mass-loss history), the carbon-oxygen core is not very degenerate and carbon ignites as it contracts, followed by a succession of nuclear reaction sequences which very quickly produce an inner iron core. Any further reactions are endothermic and cannot contribute to the luminosity of the star. Photo-disintegration of iron, combined with electron capture by protons and heavy nuclei, then removes most of the electron degeneracy pressure supporting the core and it begins to collapse rapidly. When the density becomes large enough the inner core rebounds sending a shock wave outwards through the outer layers of the star that have remained suspended above the collapsing core. As a result the envelope of the star is ejected in a SN explosion so that the AGB is truncated soon after the start of carbon burning. The remnant in the inner core stabilises to form a neutron star (NS) supported by neutron degeneracy pressure unless its mass is large enough that complete collapse to a black hole occurs.

Stars with $M_{\text{zams}} \gtrsim 25M_{\odot}$ are severely affected by mass loss during their entire evolution and may lose their hydrogen envelopes, exposing nuclear processed material. If this occurs a naked helium star is produced and such stars (or stars about to become naked helium stars) may be WR stars. WR stars are massive objects which are found near the MS, are losing mass at very high rates and show weak or no hydrogen lines in their spectra. Naked helium stars can also be produced from less massive stars in binaries as a consequence of mass transfer (see Fig. 1b). Variation in composition affects the stellar evolution timescales as well as the appearance in the HRD and even the ultimate fate of the star. A more detailed discussion of the various phases of evolution can be found in Hurley et al. (2000).

2.2 Binary evolution

The evolution of binary stars does not differ from that of single stars unless they get in each other's way. If the binary orbit is wide enough the individual stars are not affected by the presence of a companion so that standard stellar evolution theory is all that is required to describe their development. However if the stars become close they can interact, with consequences for the evolution. Models for binary evolution have been implemented in the past (e.g. Whyte & Eggleton 1985; Pols & Marinus 1994; Portegies Zwart & Verbunt 1996). Here we carry out computational simulations with the rapid-binary evolution algorithm first developed by Tout et al. (1997) and recently updated by Hurley et al. (2002). Amongst other improvements Hurley et al. (2002) incorporate the detailed single-star evolution formulae of Hurley, Pols & Tout (2000) which allow for a wider range of stellar types than the description of stellar evolution used by Tout et al. (1997). This requires an

update of the treatment of processes such as Roche lobe overflow, common-envelope evolution and coalescence by collision (the reader is referred to Hurley et al. 2002 for further details).

As a result of Roche-lobe overflow it is possible for the binary components to come into contact and coalesce or for the binary to reach a common-envelope (CE) state. The most frequent case of common-envelope evolution involves a giant transferring mass to a main-sequence star on a dynamical timescale. Although the process is difficult to model, and therefore uncertain, it is envisaged that the secondary is not able to accept the overflowing material owing to its relatively long thermal timescale. The giant envelope overfills the Roche-lobes of both stars so that the giant core and the MS star are contained within a common-envelope. Owing to its expansion the envelope rotates slower than the orbit of the core and the MS star so that friction causes them to spiral together and transfer energy to the envelope. We assume that the cores spiral-in, transferring orbital energy to the envelope with an efficiency α_{CE} , which is necessarily a free parameter due to uncertainty in its value. It is probably not a constant (Regos & Tout 1995) but generally $\alpha_{\text{CE}} \approx 1$ is used.

Throughout this paper we refer to one star as the primary, mass M_1 , and the other as the secondary (or companion), mass M_2 . At any time the primary is the star filling, or closest to filling, its Roche lobe. Numerical values of mass, luminosity and radius are in solar units unless indicated otherwise. The algorithm provides the stellar luminosity, radius, core mass, core radius, and angular momentum, for each of the component stars as they evolve. A prescription for mass loss from stellar winds is also included in the algorithm. The algorithm covers all the evolution phases from zero-age main sequence (ZAMS) up to and including the remnant stages and is valid for all masses in the range 0.1 to 100 M_\odot and metallicities from $Z = 10^{-4}$ to 0.03. This rapid binary-evolution algorithm is a natural extension of the single-star evolution algorithm. Our aim is to evolve a population of binaries according to chosen distributions of primary mass, secondary mass and orbital separation, in conjunction with a realistic birth rate function and, from this population, to calculate birth rates and expected numbers in the Galaxy for stars that explode as type Ib/c SNe, thought to be possible GRB progenitors.

2.3 Method

We first set up a grid of initial binary parameters (in the detailed single-star evolution the secondary is removed from the system) M_1 , M_2 and separation a within the limits:

$$M_1, M_2 : 0.1 \rightarrow 80.0 M_\odot \tag{1}$$

$$a : 3.0 \rightarrow 10^4 R_{\odot} \quad (2)$$

with the $n_{\chi} = 100$ grid points of parameter χ logarithmically spaced,

$$\delta \ln \chi = \frac{1}{n_{\chi} - 1} [\ln \chi_{\max} - \ln \chi_{\min}] . \quad (3)$$

For each set of initial parameters we evolve the binary system to an age of 100 Myr. If a binary system j evolves through a phase that is to be identified with a certain individual binary population i then the system makes a contribution

$$\delta r_j = S \Phi(\ln M_{1j}) \varphi(\ln M_{2j}) \Psi(\ln a_j) \delta \ln M_1 \delta \ln M_2 \delta \ln a \quad (4)$$

to the rate r_i at which that particular population is born. This rate depends on the star formation rate S , the primary mass distribution $\Phi(\ln M_1)$, the secondary mass distribution $\varphi(\ln M_2)$ and the separation distribution $\Psi(\ln a)$. A star formation rate of $S = 7.608 \text{ galaxy}^{-1} \text{ yr}^{-1}$ is used in this work which corresponds to one star with $M > 0.8 M_{\odot}$ forming in the Galaxy every year (see Hurley et al. 2002). Such a rate is in rough agreement with the birth rate of white dwarfs in the Galaxy $\approx 2 \times 10^{-12} \text{ pc}^{-3} \text{ yr}^{-1}$ (Phillips 1989), noting that only stars with $M > 0.8 M_{\odot}$ can possibly evolve to white dwarfs in the age of the Galaxy¹, and assuming an effective Galactic volume of $\approx 5 \times 10^{11} \text{ pc}^3$. The primary mass distribution $\xi(m)$ is the IMF of Kroupa, Tout & Gilmore (1993; hereafter KTG),

$$\xi(m) = \begin{cases} 0 & m \leq m_0 \\ a_1 m^{-1.3} & m_0 < m \leq 0.5 \\ a_2 m^{-2.2} & 0.5 < m \leq 1.0 \\ a_2 m^{-2.7} & 1.0 < m < \infty, \end{cases} \quad (5)$$

where $\xi(m) dm$ is the probability that a star has a mass, expressed in solar units, between m and $m + dm$. The distribution is normalized according to $\int_0^{\infty} \xi(m) dm = 1$, so that, for $m_0 = 0.1$, $a_1 = 0.29056$ and $a_2 = 0.15571$. Then $\Phi(\ln M_1) = M_1 \xi(M_1)$. If the component masses are to be chosen independently, the secondary mass distribution is then $\varphi(\ln M_2) = M_2 \xi(M_2)$. However there is observational evidence (Eggleton, Fitchett & Tout 1989; Mazeh et al. 1992; Goldberg & Mazeh 1994) to support correlated masses: $\varphi(\ln M_2) = \frac{M_2}{M_1} = q_2$, which corresponds to a uniform distribution of the mass-ratio q_2 , for $0 < q_2 \leq 1$ (the flat- q distribution). The separation distribution is taken to be $\Psi(\ln a) = \vartheta$, a constant, between the limits 3 and $10^4 R_{\odot}$. Normalization gives $\vartheta = 0.12328$.

¹ The same assumptions regarding the star formation rate have been made previously (e.g. Iben & Tutukov 1984; Han 1998; Hurley et al. 2002) facilitating comparison with these results.

2.4 Mass loss and rotation

The particular mass-loss prescriptions through the various phases, which have been found to fit the observations well, are described in detail by Hurley et al. (2000; 2002). On the GB phase and beyond we apply mass loss to the envelope according to the formula of Kudritzki & Reimers (1978), while for the AGB we apply the formulation of Vassiliadis & Wood (1993). For massive stars we model mass loss over the entire HRD using the prescription given by Nieuwenhuijzen & de Jager (1990),

$$\dot{M}_{\text{NJ}} = \left(\frac{Z}{Z_{\odot}} \right)^{1/2} 9.6 \times 10^{-15} R^{0.81} L^{1.24} M^{0.16} \text{ M}_{\odot} \text{ yr}^{-1} \quad (6)$$

for $L > 4000 L_{\odot}$, modified by the factor $Z^{1/2}$ (Kudritzki et al. 1989). Numerical values of mass, luminosity and radius are in solar units, unless otherwise specified.

For small H-envelope mass, $\mu < 1.0$, we include a Wolf-Rayet-like mass loss (Hamann & Koesterke 1998) which we have reduced to give

$$\dot{M}_{\text{WR}} = 10^{-13} L^{1.5} (1.0 - \mu) \text{ M}_{\odot} \text{ yr}^{-1} \quad (7)$$

where μ is given by

$$\mu = \left(\frac{M_{\text{env}}}{M} \right) \min \left[5.0, \max \left\{ 1.2, \left(\frac{L}{L_0} \right)^{\kappa} \right\} \right]. \quad (8)$$

Here $L_0 = 7.0 \times 10^4 L_{\odot}$ and $\kappa = -0.5$ (Hurley et al. 2000). The reduction in \dot{M}_{WR} is necessary in order to produce sufficient black holes to match the number observed in binaries (see Hurley et al. 2000).

As we plan to use the evolution routines to investigate GRB production, it is desirable to follow the stars' angular momentum. To do this we must start each star with a realistic spin on the ZAMS. A reasonable fit to the \bar{v}_{rot} MS data of Lang (1992) is given by

$$\bar{v}_{\text{rot}}(M) = \frac{330 M^{3.3}}{15.0 + M^{3.45}} \text{ km s}^{-1} \quad (9)$$

so that

$$\Omega = 45.35 \frac{\bar{v}_{\text{rot}}}{R_{\text{zams}}} \text{ yr}^{-1}. \quad (10)$$

The angular momentum is then given by

$$J_{\text{spin}} = I\Omega = kMR^2\Omega \quad (11)$$

where the constant k depends on the internal structure, e.g. $k = 2/5$ for a solid sphere and $k = 2/3$ for a spherical shell. In actual fact we find the angular momentum by splitting the star into two parts, consisting of the core (with mass M_c) and the envelope (with mass M_{env}), so that

$$J_{\text{spin}} = \left(k_2 (M - M_c) R^2 + k_3 M_c R_c^2 \right) \Omega \quad (12)$$

where $k_2 = 0.1$, based on detailed giant models which reveal $k = 0.1 M_{\text{env}}/M$, and $k_3 = 0.21$ for an $n = 3/2$ polytrope such as a white dwarf, neutron star or dense convective core. This works well for post-MS stars which have developed a dense core whose rotation is likely to have decoupled from the envelope while also representing the near uniform rotation of homogeneous MS stars which have no core. When the star loses mass its stellar wind carries off angular momentum at a rate given by

$$\dot{J} = k \dot{M} h \quad (13)$$

where $h = R^2 \Omega$. Thus

$$J_{\text{spin}}(t + \Delta t) = J_{\text{spin}}(t) - \frac{2}{3} \Delta M R^2 \Omega \quad (14)$$

when the star loses an amount of mass ΔM , where we take $k = 2/3$ because we assume that all the mass is lost uniformly at the surface of the star ie. from a spherical shell.

We also include magnetic braking for stars that have appreciable convective envelopes

$$\dot{J}_{\text{mb}} = 5.83 \times 10^{-16} \frac{M_{\text{env}}}{M} (R\Omega)^3 M_{\odot} R_{\odot}^2 \text{yr}^{-2}, \quad (15)$$

with Ω in units of years. Following Rappaport et al. (1983) we don't allow magnetic braking for fully convective stars, $M < 0.35 M_{\odot}$ but this restriction does not affect our results here.

2.5 Core collapse progenitors

Core-collapse SNe spectra may contain hydrogen absorption lines (type II) or show very weak or no hydrogen lines at all (type Ib/c) thought to indicate the lack of a hydrogen envelope around the imploding star. As in Hurley et al. (2002), we define a type Ib/c SN as one that produces a neutron star or black hole from a primary, naked helium star. All other SN progenitors that produce a neutron star or black hole are considered to be type II. The carbon-oxygen core mass M_{CO} of a SN Ib/c progenitor has a maximum value of $\max[M_{\text{Ch}}, 0.773 M_{\text{He}} - 0.35 M_{\odot}]$ (Hurley 2000; hereafter H00), where M_{He} is the initial mass of the helium star and $M_{\text{Ch}} = 1.44 M_{\odot}$ is the Chandrasekhar mass. For masses above this, a SN explosion is assumed to take place. The expression for the maximum mass of the core of a SN II progenitor is similar with M_{He} replaced by the mass of the carbon-oxygen core at the base of the asymptotic giant branch. If

$$M_{\text{CO}} > 7.0 M_{\odot} \quad (16)$$

we assume a black hole forms (Woosley 1993). The mass of the neutron star (NS) or black hole (BH) formed is then given by (H00)

$$M_{\text{NS/BH}} = 1.17 + 0.09 M_{\text{CO}} M_{\odot} \quad (17)$$

corresponding to neutron star baryonic masses in the range $1.3 M_{\odot}$ to $1.8 M_{\odot}$ and a minimum black hole mass of $1.8 M_{\odot}$.

A Wolf-Rayet stellar wind \dot{M}_{WR} is used in the stellar models when the H-envelope mass M_{env} is small $\mu < 1.0$. Stars with $\mu > 1.0$ are excluded from the Wolf-Rayet population.

We apply the condition that a star which is to be considered as a GRB progenitor must: (i) go through a Wolf-Rayet phase, as defined above, before ending its life as a type Ib/c SN; (ii) have a sufficiently massive core to form a black hole; and (iii) have enough angular momentum at the time of collapse to allow the formation of a disc. To decide whether a centrifugally supported accretion disc can form around a central black hole we compare the angular momentum of the progenitor star to that which a test particle would require at the last stable orbit (LSO) around a black hole (see e.g. Heger & Woosley 2002). In the case of a non-rotating, spherically symmetric black hole the last stable orbit has a radius $r_{\text{LSO}} = 6GM_{\text{BH}}/c^2$. The condition that the matter does not spiral into the black hole is simply that the rotational energy of the matter should be greater or equal to half the gravitational potential energy: $\frac{1}{2}J^2/I \leq \frac{1}{2}GM_{\text{BH}}m/r_{\text{LSO}}$, where J is the angular momentum of the element mass m and $I = mr_{\text{LSO}}^2$ is its moment of inertia about the hole in the LSO. In other words, $j > GM_{\text{BH}}r_{\text{LSO}}^{1/2}$, where j is the specific angular momentum $j = J/m$. The inner boundary condition is therefore that the angular momentum with which the material arrives at the stable orbit should be greater than or equal to this critical value.

3 PROGENITORS OF CORE COLLAPSE SNe AND GRBs

3.1 Supernovae

The effects of close binary evolution are observed in many systems, such as cataclysmic variables, X-ray binaries and Algols and by the presence of stars such as blue stragglers which cannot be explained by single star evolution. The fraction of star systems containing at least two gravitationally bound stars, i.e. the binary fraction, is at least 50% (see Larson 2001 for a recent review). In the case of Wolf-Rayet stars it is perhaps as high as 80%. Some uncertainty still exists due to small number statistics but multiplicity seems a crucial element of massive star evolution.

While many of the processes involved are not understood in detail we do have a qualitative

picture of how binaries evolve and can hope to construct a model that correctly follows them through the various phases of evolution. In order to conduct statistical studies of complete binary populations, i.e. population synthesis, such a model must be able to produce any type of binary that is observed in enough detail.

For most of the individual binary populations, observational birth rates or numbers in the Galaxy are uncertain because of selection effects involved when undertaking surveys. However enough data exist overall to enable a meaningful comparison with the results. Cappellaro (2001) combined the results of five independent SN searches to obtain a sample of 137 SNe from which he derived the following birth rates for the Galaxy:

$$\begin{aligned} 2.4 \pm 1 \times 10^{-3} \text{ yr}^{-1} & \quad \text{SN Ib/c} \\ 14.9 \pm 6 \times 10^{-3} \text{ yr}^{-1} & \quad \text{SN II.} \end{aligned}$$

The values reported above assume $H_0 = 65 \text{ km s}^{-1} \text{ Mpc}^{-1}$, and that the Galaxy has an average SN rate its morphological type (here assumed Sb-Sbc) and luminosity ($2.3 \times 10^{10} L_{B,\odot}$; see Cappellaro et al. 1999). Our predicted formation rates for SNe Ib/c and SNe II in single and binary stellar populations are shown in Table 1. Binary models have been evolved according to chosen distributions of primary (KTG distribution) and secondary (KTG or q-flat distribution) masses. Throughout this paper we refer to these distributions as KTG-KTG or KTG-q, respectively. The single star results are consistent with the observed rates, as are the binary type II SNe at $Z = 0.02$. A discrepancy lies in the birth rates of type Ib/c SNe because the theoretical rates in the KTG-q case are high but not for the KTG-KTG case which are in good agreement. This can be reconciled by assuming a binary fraction smaller than unity (Hurley et al. 2002).

The SN II rate is a fairly robust number but the SN Ib/c rate is sensitive to many of the assumptions underlying the model (Hurley et al. 2002). In binary models the majority of type Ib/c SNe come from naked helium stars formed from relatively low-mass progenitors ($10 - 20 M_{\odot}$) stripped by the interaction, while single SNe Ib/c arise mainly from more massive stars $> 24 M_{\odot}$ which become Wolf-Rayet stars prior to explosion (see Fig. 2a). In a model containing only single stars with $Z = 0.02$ the SN Ib/c rate is reduced to $2 \times 10^{-3} \text{ yr}^{-1}$ which would be consistent with observations. These rates are sensitive to the assumed mass-loss rate for red supergiants (see Hurley et al. 2000), as well as to our assumption that black hole formation ignites a SN explosion, both of which are very uncertain. If mass-loss rates are lower or if black holes form without a SN, the SN Ib/c rate from single stars would be lower.

3.2 Gamma-ray bursts

GRBs are thought to be produced when the evolved core of a massive star collapses to a black hole and the remaining star has too much angular momentum to fall in directly. Using the rapid binary code we are able to generate a series of large single and binary populations and evaluate the formation rate of interesting core collapse species. Rotating naked helium stars, presumed to have lost their envelopes to winds or companions, are evolved from the ZAMS ignition up to the formation of the final CO core.

The cumulative rate (above a threshold core mass, M_{CO}) for stars of $Z = Z_{\odot}$ that explode as type Ib/c SNe is shown in Fig. 2a. A fraction, f_{BH} , of the above stars will form a central black hole after exploding (see Fig. 2b). By including angular momentum transport by non-magnetic processes, such as mass loss, mass transfer and mass accretion, we are able to roughly estimate the fraction f_{Ω} of SN Ib/c progenitors that end their lives with sufficient angular momentum to form a centrifugally supported disc (see Fig. 2c).

High angular momentum is a common requirement in all current GRB models that involve massive stars, including those that use a pulsar power source. Yet the actual angular momentum in a presupernova star is unknown. Without magnetic fields, and with our approximate treatment of angular momentum transport, we find that a naked helium star cannot retain enough angular momentum to form a centrifugally supported disc around the collapsed object, as required by the collapsar model of GRBs ($f_{\Omega} \approx 0$ for single stars; see Fig. 2c). The main reason is that during the early phase of WR evolution, the progenitor star spins down significantly as it loses a large fraction of its mass quite rapidly (Fig. 3). This is even more so if magnetic fields couple the core effectively to the envelope – the magnetic interaction of the rapidly rotating helium core with its stationary envelope during the red supergiant phase will halt the core, making it unfit as a collapsar progenitor (Spruit & Phinney 1998; Spruit 2002; Heger & Woosley 2002; but see Livio & Pringle 1998). Either the description of the stellar model is inaccurate or some route other than single star evolution must be involved in making GRBs. The natural alternative is a close binary.

If either star fills its Roche lobe, then gas flows from the outer layers of the star through the inner Lagrangian point that connects the two Roche lobes. Some or all of this gas may be captured by the companion star so that mass transfer occurs and, as a result, the subsequent evolution of both stars takes a different course from that of isolated stars with important consequences for their orbit and spin (Fig. 4). If the hydrogen envelope is removed too early (or the two stars coalesce) mass loss from the WR star also reduces the angular momentum (Fig. 5). The effect that the com-

panion mass has on the outcome of binary evolution is illustrated by comparing the evolution of the primary star in Figs. 4 and 5.

Finally, the expected birth rates of stars in the Galaxy that have both a massive enough core to form a black hole and an adequate rotation rate at the time of collapse to allow the formation of a disc are shown in Fig. 2d. These core collapse species may be the progenitors of the common (long-soft) GRBs.

3.3 Sensitivity to model parameters

To give an idea of how sensitive the final state of the system is to changes in the physical parameters that govern the evolution, we reconsider the example illustrated in Fig. 2. If the common-envelope efficiency of the component stars is taken to be $\alpha_{\text{CE}} = 3$, rather than $\alpha_{\text{CE}} = 1$, less energy is required to drive off the common envelope. The result is similar to a reduction in the envelope binding energy and so it is less likely that the process ends in coalescence of the cores. This increment in the common-envelope efficiency parameter slightly increases the GRB production rate (see Fig. 6). Wider systems are not brought within an interaction distance after the common-envelope phase. Thus systems that do interact when $\alpha_{\text{CE}} = 1$ do not do so when $\alpha_{\text{CE}} = 3$. However, the net increase is mainly because closer systems that would coalesce when $\alpha_{\text{CE}} = 1$ now remain detached.

At first sight this may seem an unphysical model given the definition but, as discussed by Iben & Livio (1993), an increase in α_{CE} can be possible if additional energy sources other than the orbital energy are involved. Processes with potential to supply such energy include enhanced nuclear burning in shell burning zones of giants, nuclear burning on the surface of a degenerate secondary, dynamo generation of magnetic fields and recombination of the hydrogen and helium ionization zones in giants. Possibly the common envelope absorbs ordinary nuclear energy in the process of swelling up, but this should occur on a thermal timescale. Unfortunately, the theoretical determination of reliable values for α_{CE} has proven difficult owing to a lack of understanding of the processes involved and our inability to model them.

An increase (or decrease) of the mass-loss rate has profound consequences for the WR population. At a given metallicity, the minimum initial mass for the formation of a WR star (lower for higher \dot{M}), the duration of the WR stage (greater for higher \dot{M}), the times spent in the different WR subtypes and the surface composition during these phases are all very sensitive to the mass-loss rates (Maeder 1991). There is no doubt that major changes to the outcome result if \dot{M}_{WR} is

altered by even a small fraction f_M . Inspection of Fig. 7 reveals that as the mass-loss is reduced, the threshold for the removal of the hydrogen envelope by stellar winds is raised and the loss of angular momentum is inhibited. This increases the mass of the CO core and favours black hole formation. Conversely, increasing the mass-loss rate promotes the loss of angular momentum and inhibits black hole formation (see Fig. 7).

It should be noted that the choice of the initial mass above which stars become black holes rather than neutron stars is not well constrained. The low-mass X-ray binary (LMXB) catalogue compiled by van Paradijs (1995) lists about 80 bright persistent sources in the Galaxy but makes no distinction as to whether the compact star is a neutron star or black hole. While this number is in fair agreement (H00) with the birth rates derived with the prescription for the remnant's mass given in equation (17), the differences introduced by this choice in the overall evolution are small when compared with those resulting from varying the (very uncertain) initial distributions. The birth rate of persistent neutron star LMXBs derived by means of such a prescription is similar to the rate found by Portegies Zwart et al. (1996) in their standard model that includes velocity kicks. Measurements of black hole masses in binaries, although still highly uncertain, yield values between 3 and $20M_\odot$ (Orosz et al. 2001; McClintock et al. 2001; Froning & Robinson 2001; Wagner et al. 2001; Table 1 of Fryer & Kalogera 2001 and references therein). For progenitors of $40 \leq M_{\text{zams}}/M_\odot \leq 100$, equation (17) gives final remnant masses in the range $1.8 - 3.0M_\odot$ (Fig. 8). If the amount of mass that a black hole can accrete is limited by the Eddington limit (Cameron & Mock 1967) then a black hole is unlikely to accrete enough material to take its mass above $5M_\odot$ and this model is inconsistent with the observations. There is, however, some uncertainty as to whether the Eddington limit should actually be applied because the energy generated in excess of the limit might be removed from the system in a strong wind or asymmetrically through a disc. Super-Eddington accretion rates may be crucial in allowing black holes in binaries to gain a significant amount of mass.

Imposing the Eddington limit significantly reduces our ability to grow black hole masses to the observed values and, for this reason, in addition to our somewhat arbitrary prescription (see equation 17) for neutron star and black hole masses, we also use the formalism developed by Belczynski, Kalogera & Bulik (2002b; hereafter B02). Based on the Hurley et al. (2000) formulae, they calculate the final CO core of a star and then use stellar models of Woosley (1986) to obtain a final FeNi core mass as a function of the CO core mass (see their equation [1]). To estimate the mass of the remnant formed, B02 follow the results of hydrodynamical core-collapse calculations (Fryer et al. 1999; Fryer & Kalogera 2001). Fig. 9 compares the black hole birth rates derived

using the B02 formalism with those based on equation (17). The birth rate of black holes shows an increase for stars with low CO core masses. Comparing the birth rates of GRBs in both models reveals a variation by a factor of 5. The relevance of the relative distribution of neutron stars and black holes on the birth rates of GRBs is further complicated by the fact that a rapidly rotating neutron stars with an ultrahigh magnetic field could, in principle, also serve as a trigger (Usov 1992; Thompson 1994).

These examples serve to demonstrate the sensitivity of binary evolution to the choice of model parameters.

3.4 Stellar companions

One of the most important questions relating to WR stars is whether they are all members of binary systems or rather do some truly single objects exist. Possibly the majority of stars are members of binary or multiple systems but most are sufficiently far from their companions that their evolution proceeds essentially as if they were single stars. However there is an important minority of stars which are close enough that their evolution is dramatically changed by the presence of a companion. The most dramatic effects occur when one of the stars in the system is a very compact object. Here we investigate the expected binary systems with black hole primaries which may be the sources of GRBs earlier in their evolution.

Table 2 shows the various types of companions to the GRB progenitor star at the time of collapse. For both secondary mass distributions the vast majority of companions are, without surprise, MS stars and thus likely donors of soft X-ray binaries (Lee et al. 2002). The typical orbital periods for these binaries at the time of explosion are in the 0.01 – 1 days range (Fig. 10). Most companions, being MS stars, have small mass-loss rates of $10^{-8} M_{\odot} \text{yr}^{-1}$ or less and are thus unlikely to significantly enhance the density around the GRB progenitor. There is a small, interesting sub-class of binaries in which the companion star is a collapsed object (about 1% for the KTG-q distribution). In this case, the GRB, which is likely caused by the relativistic jet, expelled along the rotation axis of the collapsing stellar core, propagates within a SN remnant of about 1 Myr in age.

4 THE ROLE OF METALLICITY

The assumption that all stars within the population are born with the same composition is somewhat naive: nucleosynthesis in successive generations of stars enriches the gas from which they

form as the Galaxy evolves. Metallicity Z influences the stellar evolution of massive stars mainly through bound-free and line opacities in the outer layers of massive stars owing to their influence on stellar wind mass loss rates. The numbers of WR stars in galaxies of different metallicities are an important test of the stellar models at various Z and of the values of the final stellar masses. The theoretical predictions of the ratios of WR/O-stars, WC/WR and WC/WN are in good agreement with observations of the Local Group (Maeder 1991), which support the following dependence of the mass-loss rates on metallicity: $(\dot{M}_z/\dot{M}_\odot) = (Z/Z_\odot)^{0.5}$ (de Jager et al. 1988).

From our large binary population models with a variety of initial masses and metallicities we find that both the fraction of stars that form a central black hole and those that end their lives with sufficient angular momentum to form a disc significantly increase with decreasing metallicity (Figs. 11 – 13). This is because low metallicity keeps the radius of the star smaller and reduces mass loss. Both properties inhibit the loss of angular momentum (MacFadyen & Woosley 1999; Heger & Woosley 2002) so low- Z stars are likely to be rotating more rapidly. Also, the lower the metallicity, the higher the stellar mass for WR star formation. The latter increases the mass of the heaviest CO core and favours black hole formation which in turn could power a more luminous burst because more energy can be extracted from the black hole via e.g. the Blandford-Znajek mechanism (Blandford & Znajek 1977; Lee et al. 2000; Wheeler, Meier & Wilson 2002).

The likely metallicity dependence of both black-hole formation and rotation suggests that the production of GRBs is likely to be affected by the physical conditions in the local ISM – at high Z gas opacities are larger in the outer stellar layers and so more momentum is transferred by radiation pressure, mass-loss is more intense and GRB formation is disfavoured.

What are the effects of a dependence of GRB luminosity on the metallicity of their progenitors? The most significant is a potential offset between the true star-formation rate and that traced by GRBs (Ramirez-Ruiz, Lazzati & Blain 2002). If GRBs in low-metallicity environments and in low-mass galaxies are more luminous then they are likely to be overrepresented in GRB samples. Low-mass galaxies are likely to have statistically lower metallicities and thus contain more luminous GRBs than high-mass galaxies. Because galaxy mass is expected to build up monotonically through mergers, it is possible that the highest- z GRBs could be systematically more luminous due to the lower mass of their hosts. This effect is likely to be more significant than, but in the same direction as, the global increase in metallicity with cosmic time.

The most luminous GRBs of all could be associated with metal-free Population-III stars but

their very high redshifts would make examples difficult to find even in the *Swift*² catalogue of hundreds of bursts.

Star-formation activity is likely to be enhanced in merging galaxies. In major mergers of gas-rich spiral galaxies this enhancement takes place primarily in the inner kpc, as bar instabilities drive gas into the core (Mihos & Hernquist 1994). Metallicity gradients in the gas are likely to be smoothed out both by mixing prior to star formation and by SN enrichment during the burst of activity. GRB luminosities could be suppressed in such well-mixed galaxies making GRBs more difficult to detect in these most luminous objects.

Shocks in tidal tails associated with merging galaxies are also likely to precipitate the formation of high-mass stars, yet as such tails are likely to consist of relatively low-metallicity gas, it is perhaps these less intense sites of star-formation at large distances from galactic radii that are more likely to yield detectable GRBs. This might have the unfortunate consequence of making GRBs more difficult to use as clean markers of high- z star-formation activity. More optimistically, the astrophysics of star formation in high-redshift galaxies could be studied using the intrinsic properties of a well-selected population of GRBs with deep, resolved host galaxy images. If there is a bias towards the discovery of GRBs in low-metallicity regions, then the GRB host galaxy luminosity function will be biased to low luminosities.

5 COMPARISON WITH OBSERVATIONS

The high Lorentz factors and energies seen in GRBs are consistent with the catastrophic formation of a stellar black hole with mass of a few M_{\odot} , with about 1 % of the rest mass energy going to a relativistic outflow. This could be the extreme example of the asymmetric explosion produced by supernovae (Khokhlov et al. 1999) in which, instead of halting at the neutron star stage, the collapse continues to the black-hole stage producing an even faster jet in the process (MacFadyen & Woosley 1999). GRBs arising from a small fraction of stars that undergo this type of catastrophic energy release are likely to produce collimated outflows.

Even if the outflow is not highly collimated some beaming is expected because energy would be channeled preferentially along the rotation axis. Also, one would expect baryon contamination to be lowest near the axis because angular momentum flings material away from the axis and material with low-angular momentum falls into the black hole. The dynamics, however, are complex.

² <http://swift.gsfc.nasa.gov>

While numerical simulations of collapse scenarios can address the fate of the bulk of the matter (MacFadyen & Woosley 1999; MacFadyen, Woosley & Heger 2001; Aloy et al. 2000, 2002; Zhang et al. 2003), higher resolution simulations of the outer layers of the stellar mantle seem to be required because even a very small number of baryons polluting the outflow could severely limit the attainable Lorentz factor. The entrained baryonic mass would need to be below $10^{-4} M_{\odot}$ to allow these high relativistic expansion speeds.

Although jets in GRBs were first suggested for GRB 970508 (Waxman, Kulkarni & Frail 1998), they were widely invoked for GRB 990123 to explain its spectacular energy release. Subsequent multi wavelength observations of GRBs have been interpreted as evidence for explosions with jet-like geometry (Stanek et al. 1999; Harrison et al. 1999; Castro-Tirado et al. 1999). The detection of polarization (e.g., Covino et al. 1999; Wijers et al. 1999) gave further credence to the jet hypothesis.

Because conical fireballs are visible to only a fraction f_b of observers, the true GRB rate is $R_t = \langle f_b^{-1} \rangle R_{\text{obs}}$ where R_{obs} is the observed GRB rate and $\langle f_b^{-1} \rangle$ is the mean of the beaming fractions. Frail et al. (2001) recently derived $\langle f_b^{-1} \rangle \approx 500$ for a comprehensive sample of GRB afterglows with known distances based on observed broadband breaks in their light curves³. This implies, within the uncertainties and possible limitations of such a method, that only a small fraction of GRBs are visible to a given observer and therefore the true GRB rate is several hundred times larger than the observed one: $R_{\text{obs}} \approx 10^{-5} R_{\text{SN Ib/c}}$ (Schmidt 2001). Fig. 14 shows our formation rates (as a function of Z) for GRB progenitors, stars that have both a massive enough core to form a black hole and adequate rotation at the time of collapse to allow the formation of a disc. Clearly these rates are highly sensitive to the assumed black hole formation model. Binary models in the KTG-q case are easily capable of supplying a sufficient number of progenitors even if the GRB rate is several hundred times larger than the observed rate. A discrepancy lies in the birth rates of collapsars when using an initial KTG-KTG distribution of binaries because the theoretical rates in the H00 case are low but not for the B02 case which are in good agreement. This can be reconciled by assuming a smaller mass threshold for black hole formation (see equation 16).

³ This estimate assumes that the breaks observed in many GRB afterglow lightcurves are due to a geometrical beam effect and not to either a transition to non-relativistic expansion or an environmental effect such as a sharp density gradient. An important feature produced by this jet collimation is the achromaticity of the afterglow break, which clearly distinguishes it from the steepening that may be produced by the passage of a spectral break through the observing band.

6 CONCLUSIONS

The primary purpose of this paper was to use the rapid binary-evolution algorithm to evaluate the formation rate of interesting individual species of WR stars that may be the progenitors of the common long-soft GRBs. Rotating naked helium stars, presumed to have lost their envelopes in winds or to companions, are followed from the ZAMS up to the formation of the CO core. Recognizing that the two essential ingredients for the collapsar model are a sufficiently massive core to form a black hole and enough rotation to form a disc, we have studied their effects on the results of binary populations synthesis and made a global comparison with GRB observations.

The framework we have used to determine a star's angular momentum is a simple one. While many of the processes involved are not understood in detail, we do have a qualitative picture of how binaries evolve and we hope to construct a model that correctly follows them through the various phases of evolution. This method has led us to conclude that the resulting spin rates for single stars become too low to form a centrifugally supported disc to drive a GRB engine. Heger & Woosley (2002), including more realistic estimates of angular momentum transport, argue that some single stars may still be able to form a disc. However inclusion of magnetic torques in their calculations also results in too little angular momentum for collapsars. Either the stellar model description is inaccurate or some other evolutionary path must be involved in making GRBs. The obvious option is a close binary or merger (see also Fryer et al. 1999), where tidal interaction transfers orbital angular momentum to the stellar rotation. An important ingredient is the fact that the rapidly rotating new black holes that power the GRBs are typically accompanied by MS stars and so are likely donors of soft X-ray binaries (only those MS stars which remained gravitationally bound after the explosion).

For most of the individual binary populations we find that the expected formation rates of collapsars in the Galaxy are easily capable of supplying a sufficient number of progenitors, even if the true GRB rate is several hundred times larger than the observed rate because of beaming. An interesting conclusion of this work is that binary stars at low metallicity are important for the formation of a rapidly rotating, massive helium core at collapse. This effect could increase the GRB formation rates by a factor of 5–7 at $Z = Z_{\odot}/200$. We finally note that the simple binary-evolution algorithm provides an adequate description of the observations although more stringent constraints to many of the evolution variables are needed in order to draw more accurate conclusions.

ACKNOWLEDGMENTS

We are grateful to M. J. Rees, P. Podsiadlowski, A. MacFadyen and J. Hurley for helpful conversations. We also thank the referee, K. Belczynski, for comments that led to improvements of this paper. ER-R acknowledges patronage from CONACYT, SEP and the ORS foundation. RGI thanks PPARC for support. CAT thanks Churchill College for a fellowship.

REFERENCES

- Aloy M. A., Ibanez J. M., Marti J. M., Muller E., MacFadyen A. I., 2000, *ApJ*, 531, L119
- Aloy M. A., Ibanez J. M., Miralles J. A., Urpin V., 2002, *A&A*, 396, 693
- Belczynski K., Bulik T., Rudak B., 2002a, *ApJ*, 571, 394
- Belczynski K., Kalogera V., Bulik T., 2002b, *ApJ*, 572, 407 (B02)
- Blandford R. D., Znajek R., 1977, *MNRAS*, 179, 433
- Bombaci I., 1996, *A&A*, 305, 871
- Cameron A.G.W., Mock M., 1967, *Nature*, 215, 464
- Cappellaro E., Evans R., Turatto M., 1999, *A&A*, 351, 459
- Cappellaro E., 2001, *Mem. S. A. It.*, vol 72-4, 863
- Castro-Tirado A. J. et al., 1999, *Science*, 283, 5410
- Costa E. et al., 1997, *Nature*, 387, 783
- Covino S. et al., 1999, *A&A*, 348, L1
- de Jager, C., Nieuwenhuijzen, H. & van der Hucht, K., 1988, *A&AS*, 72, 259
- Eggleton P.P., Fitchett M., Tout C.A., 1989, *ApJ*, 347, 998
- Frail D. A., Kulkarni S. R., Nicastro S. R., Feroci M., Taylor G. B., 1997, *Nature*, 389, 271
- Frail D. A. et al., 2001, 562, L55
- Froning C. S., Robinson E. L., 2001, *AJ*, 121, 2212
- Fryer C. L., Woosley S. E., 1998, *ApJ*, 502, L9
- Fryer C. L., Woosley S. E., Hartmann D. H., 1999, *ApJ*, 526, 152
- Fryer C. L., Kalogera V., 2001, *ApJ*, 554, 548
- Fryer C. L., Woosley S. E., Heger A., 2001, *ApJ*, 550, 372
- Goldberg D., Mazeh T., 1994, *A&A*, 282, 801
- Hamann W.-R., Koesterke L., 1998, *A&A*, 335, 1003
- Han Z., 1998, *MNRAS*, 296, 1019
- Harrison F. A. et al., 1999, *ApJ*, 523, L121
- Heger A., Woosley S. E., 2002, *astro-ph/0206005*
- Hurley J. R., 2000, Ph.D. thesis, Cambridge Univ
- Hurley J. R., Pols O.R., Tout C.A., 2000, *MNRAS*, 315, 543
- Hurley J. R., Tout C.A., Pols O.R., 2002, *MNRAS*, 329, 897
- Iben I.Jr, Tutukov A. V., 1984, *ApJS*, 54, 335
- Iben I.Jr., Livio M., 1993, *PASP*, 105, 1373
- Khokhlov A. M. et al., 1999, *ApJ*, 529, L107
- Kluźniak W., Lee W. H., 1998, *ApJ*, 494, L53
- Kroupa P., Tout C.A., Gilmore G., 1993, *MNRAS*, 262, 545
- Kudritzki R.P., Reimers D., 1978, *A&A*, 70, 227

- Kudritzki R.P., Pauldrach A., Puls J., Abbott D.C., 1989, A&A, 219, 205
- Lang K.R., 1992, *Astrophysical Data*, Springer-Verlag
- Larson R. B., 2001, in Zinnecker, H. and Mathieu R. D. eds., IAU 200 Symposium
- Lee H. K., Wijers R. A. M. J., Brown G. E., 2000, PhR, 325, 83
- Lee H. K., Brown G. E., Wijers R. A. M. J., 2002, ApJ, 575, 996
- Lee W. H., Ramirez-Ruiz E., 2002, ApJ, 577, 893
- Livio M., Pringle J. E., 1998, ApJ, 505, 339
- Maeder A., 1991, A&A, 242, 93
- MacFadyen A. I., Woosley S. E., 1999, ApJ, 524, 262
- MacFadyen A. I., Woosley S. E., Heger A., 2001, ApJ, 550, 410
- Matzner C. D., 2003, MNRAS, 345, 575
- Mazeh T., Goldberg D., Duquennoy A., Mayor M., 1992, ApJ, 401, 265
- McClintock J. E., Garcia M. R., Caldwell N., Falco E. E., Garnavich P. M., Zhao P., 2001, ApJ, 551, 147
- Mészáros P., 2001, Science, 291, 79
- Mészáros P., Rees M. J., 2001, ApJ, 2001, ApJ, 556, L37
- Mészáros P., Waxman E., 2001, Phys. Rev. Lett., 87, 1102
- Mihos J. C., Hernquist L., 1994, 431, L9
- Nieuwenhuizen H., de Jager C., 1990, A&A, 231, 134
- Orosz J. A. et al., 2001, ApJ, 555, 489
- Phillips J. P., in Torres-Peimbert S. ed., Planetary Nebulae. IAU 131 Symposium, (Kluwer:Dordrecht), 425
- Pols O.R., Marinus M., 1994, A&A, 288, 475
- Portegies Zwart S.F., Verbunt F., 1996, A&A, 309, 179
- Ramirez-Ruiz E., Dray L., Madau P., Tout C. A., 2001, MNRAS, 327, 829
- Ramirez-Ruiz E., Lazzati D., Blain A. W., 2002, ApJ, 565, L9
- Ramirez-Ruiz E., Celotti A., Rees M. J., 2002, MNRAS, 337, 1349
- Rappaport S., Verbunt F., Joss P., 1983, ApJ, 275, 713
- Regős E., Tout C.A., 1995, MNRAS, 273, 146
- Ruffert M., Janka H.-T., 1999, A&A, 344, 573
- Schmidt M., 2001, ApJ, 552, 36
- Soderberg A. M., Ramirez-Ruiz E., 2002, MNRAS, 330 L24
- Spruit H. C., Phinney E. S., 1998, Nature, 393, 193
- Spruit H. C., 2002, A&A, 381, 923
- Stanek K. Z., Garnavich P. M., Kaluzny J., Pych W., Thompson I., 1999, ApJ, 522, L39
- Thompson C., 1994, MNRAS, 270, 480
- Tout C.A., Aarseth S.J., Pols O.R., Eggleton P.P., 1997, MNRAS, 291, 732
- Usov V. V., 1992, Nature, 357, 472
- van Paradijs J., 1995, in Lewin W.H.G., van Paradijs J., van den Heuvel E.P.J., eds., X-ray Binaries. Cambridge Astrophysics Series, 26, p. 520
- van Paradijs et al., 1997 Nature, 386, 686
- Vassiliadis E., Wood P.R., 1993, ApJ, 413, 641
- Wagner R. M., Foltz C. B., Shahbaz T., Casares J., Charles P. A., Starrfield S. G., Hewett P., 2001, ApJ, 556, 42
- Waxman E., Kulkarni S. R., Frail D. A., 1998, ApJ, 497, 288
- Wheeler J. G., Yi I., Hoflich P., Wang L., 2000, ApJ, 537, 810
- Wheeler J. C., Meier D. L., Wilson J. R., 2002, ApJ, 568, 807
- Whyte C.A., Eggleton P.P., 1985, MNRAS, 214, 357
- Wijers R. A. M. J. et al., 1999, ApJ, 523, L33

Woosley S. E., 1986, in *Nucleosynthesis and Chemical Evolution*, ed. B. Hauck et al. (Geneva: Geneva Obs.), 1

Woosley S. E., 1993, *ApJ*, 405, 273

Zhang W., Woosley S. E., MacFadyen A. I., 2003, *ApJ*, 586, 356

$Z = 0.02 = Z_{\odot}$	SN Ib/c	SN II
Single Stars	$2 \times 10^{-3} \pm 1$	$17 \times 10^{-3} \pm 4$
KTG - KTG	$1 \times 10^{-3} \pm 1$	$11 \times 10^{-3} \pm 4$
KTG - q	$6 \times 10^{-3} \pm 2$	$10 \times 10^{-3} \pm 4$

Table 1. Model rates of type Ib/c and type II SNe (per Galaxy per year) for single stars and binaries with the secondary chosen either from the KTG or q IMF. SN rates include binaries which may have coalesced or broken up. The associated uncertainties in the observed offsets represent the 1σ confidence region as calculated from the Poisson errors. $S = 7.608 \text{ Galaxy}^{-1} \text{ yr}^{-1}$ is the rate of star formation.

Stellar Type	KTG / per cent	q / per cent
Low Mass Main Sequence $M < 0.7 M_{\odot}$	77 ± 0.5	$(9.0 \pm 0.1) \times 10^{-1}$
Main Sequence $M > 0.7 M_{\odot}$	24 ± 0.1	95 ± 0.4
Hertzsprung Gap	$(1.2 \pm 0.2) \times 10^{-3}$	$(1.3 \pm 0.2) \times 10^{-1}$
Core Helium burning	$(4.4 \pm 0.3) \times 10^{-4}$	$(4.3 \pm 0.3) \times 10^{-1}$
Naked Helium Star MS	$(2.5 \pm 0.1) \times 10^{-3}$	1.2 ± 0.1
Naked Helium Star HG	$(7.6 \pm 0.3) \times 10^{-3}$	1.4 ± 0.1
Carbon-Oxygen White Dwarf	$(2.8 \pm 0.9) \times 10^{-3}$	$(1.2 \pm 0.5) \times 10^{-1}$
Oxygen-Neon White Dwarf	$(3.9 \pm 1.2) \times 10^{-3}$	$(9.9 \pm 3.4) \times 10^{-2}$
Neutron Star	$(9.5 \pm 0.4) \times 10^{-3}$	$(7.5 \pm 0.4) \times 10^{-1}$
Black Hole	$(2.6 \pm 0.2) \times 10^{-4}$	$(1.3 \pm 0.1) \times 10^{-1}$
NS/BH combined	$(9.7 \pm 0.5) \times 10^{-3}$	$(8.8 \pm 0.6) \times 10^{-1}$

Table 2. Stellar type of the companion star when the primary explodes as a possible GRB (percentages) for $Z = Z_{\odot}$ in the binary phase.

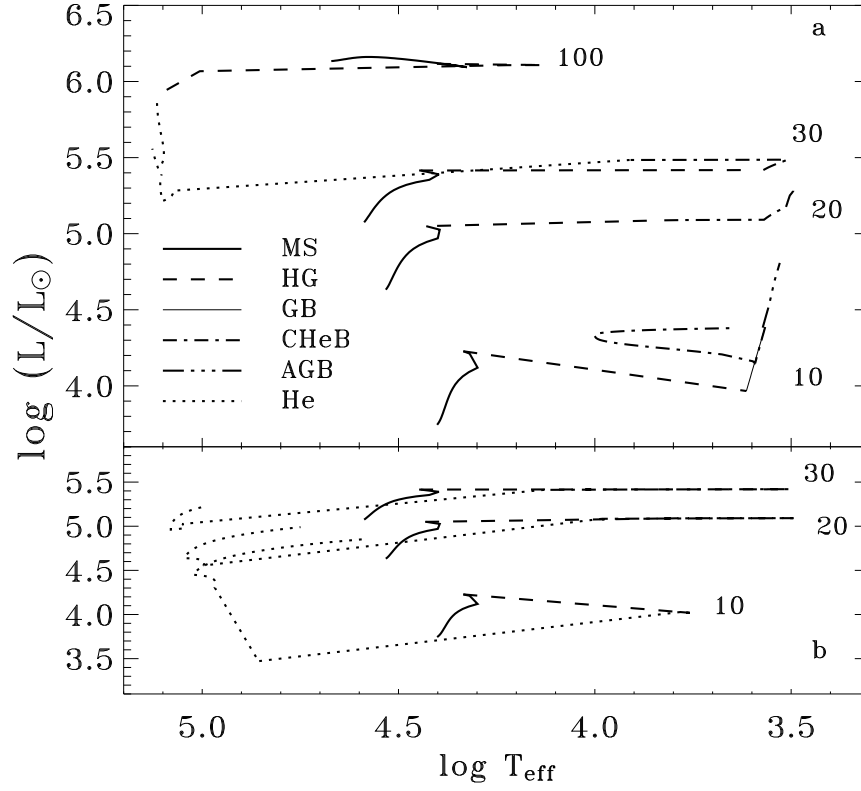


Figure 1. Selected evolutionary tracks in the HR diagram of massive stars ($M \geq 10M_{\odot}$) with initial $Z = 0.02$ composition. The different line styles correspond to different evolutionary phases: main sequence (MS); Hertzsprung gap (HG); first giant branch (GB); core helium burning (CHeB); asymptotic giant branch (AGB); and naked helium star (He). (a) Single stars evolved with mass loss by stellar winds. (b) Binary evolution with a secondary $10M_{\odot}$ star initially orbiting the primary with a 100 days period.

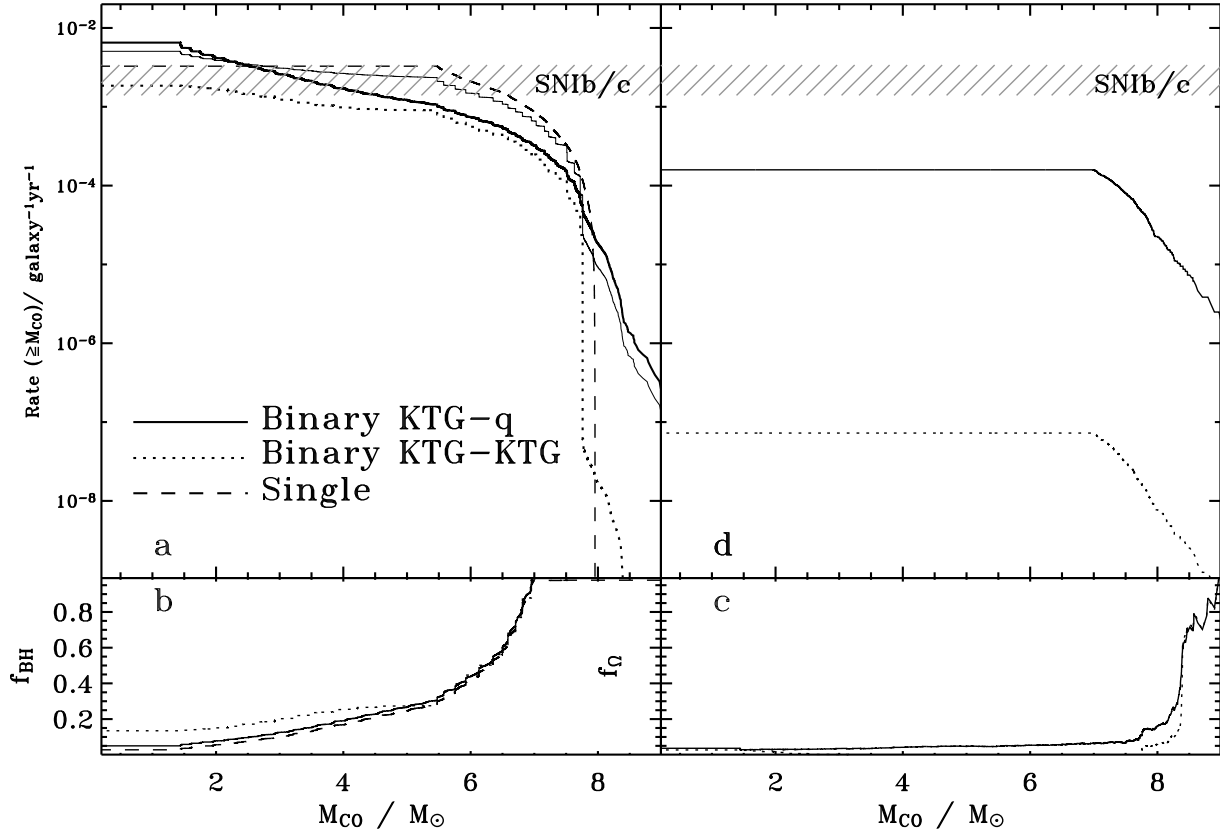


Figure 2. Formation rates of interesting core collapse species. (a) Cumulative rate (above a threshold core mass M_{CO}) for $Z = Z_{\odot}$ stars that explode as type Ib/c SNe. The shaded region represents the 1σ uncertainties on the birth rates of type Ib/c SNe as derived by Cappellaro (2001). The birth rates reported above assume $H_0 = 65 \text{ km s}^{-1} \text{ Mpc}^{-1}$, and that the Galaxy has an average SN rate for its morphological type (here assumed Sb-Sbc) and luminosity ($2.3 \times 10^{10} L_{B,\odot}$). The thin solid line assumes a 50% binary fraction (KTG-q case). (b) Fraction of SN Ib/c ($\geq M_{\text{CO}}$) that form a central black hole after exploding. (c) Fraction of SN Ib/c ($\geq M_{\text{CO}}$) that end their lives with sufficient angular momentum to form a centrifugally supported disc. (d) Cumulative rate ($\geq M_{\text{CO}}$) of stars – thought to be GRB progenitors – that have both a massive enough core to form a black hole and adequate rotation rate at the time of collapse to allow the formation of a disc.

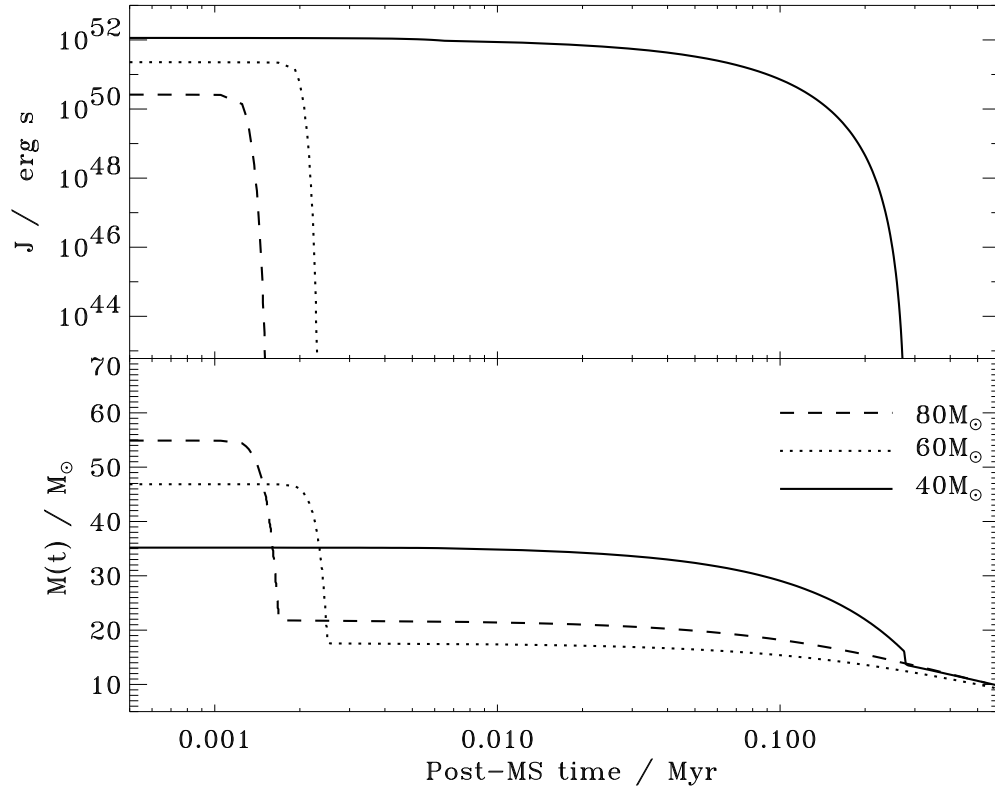


Figure 3. Single stellar evolution after core hydrogen burning for $Z = Z_{\odot}$ and initial masses $40, 60, 80 M_{\odot}$. Both the mass and angular momentum are shown for the post-MS phase as a function of time.

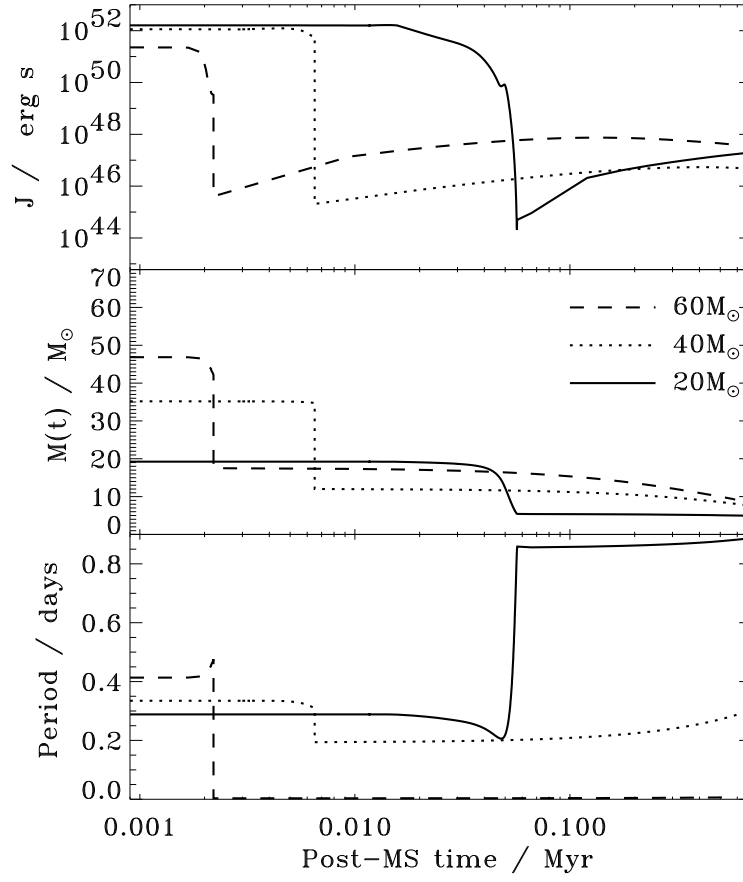


Figure 4. The evolution of the mass and angular momentum of various primary stars after core hydrogen burning for $Z = Z_{\odot}$ and initial masses 20, 40, 60 M_{\odot} with a binary companion with initial $P=100$ days and $M_2 = 10M_{\odot}$.

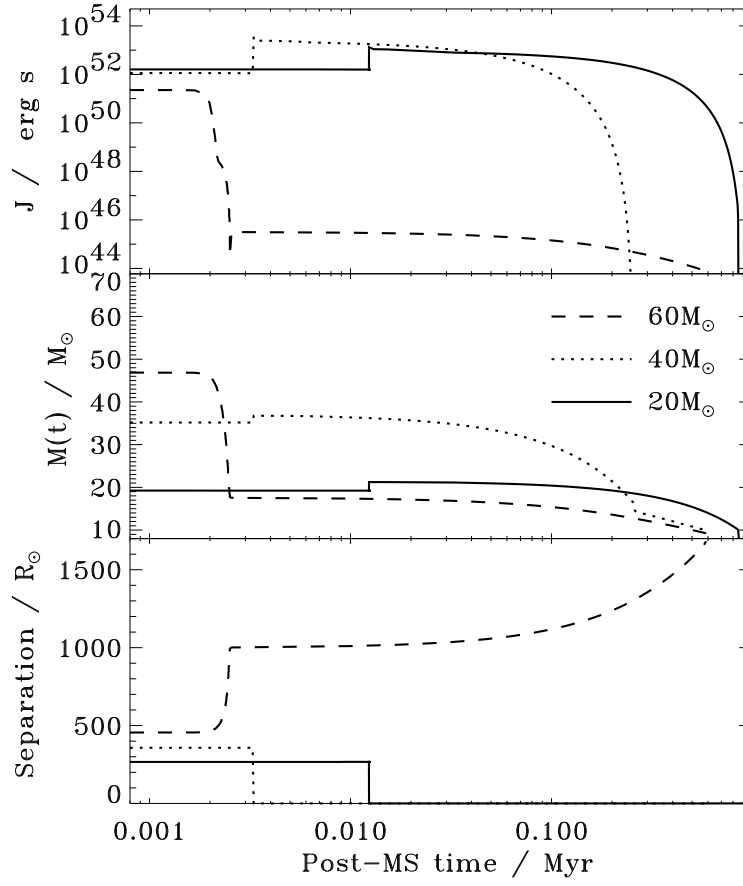


Figure 5. Similar to Fig. 4 but with $M_2 = 3M_{\odot}$.

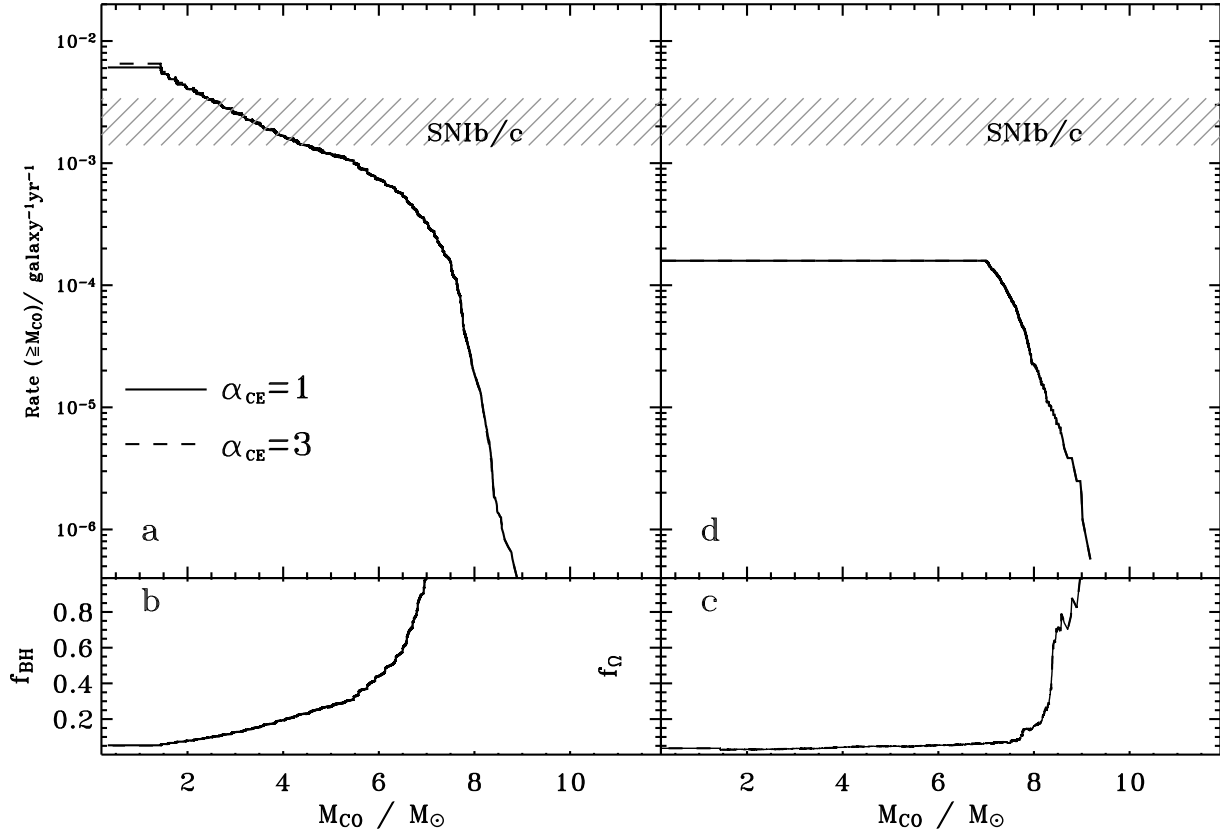


Figure 6. Similar to Fig. 2 but with $\alpha_{\text{CE}} = 3$ using an initial KTG-q distribution of binaries.

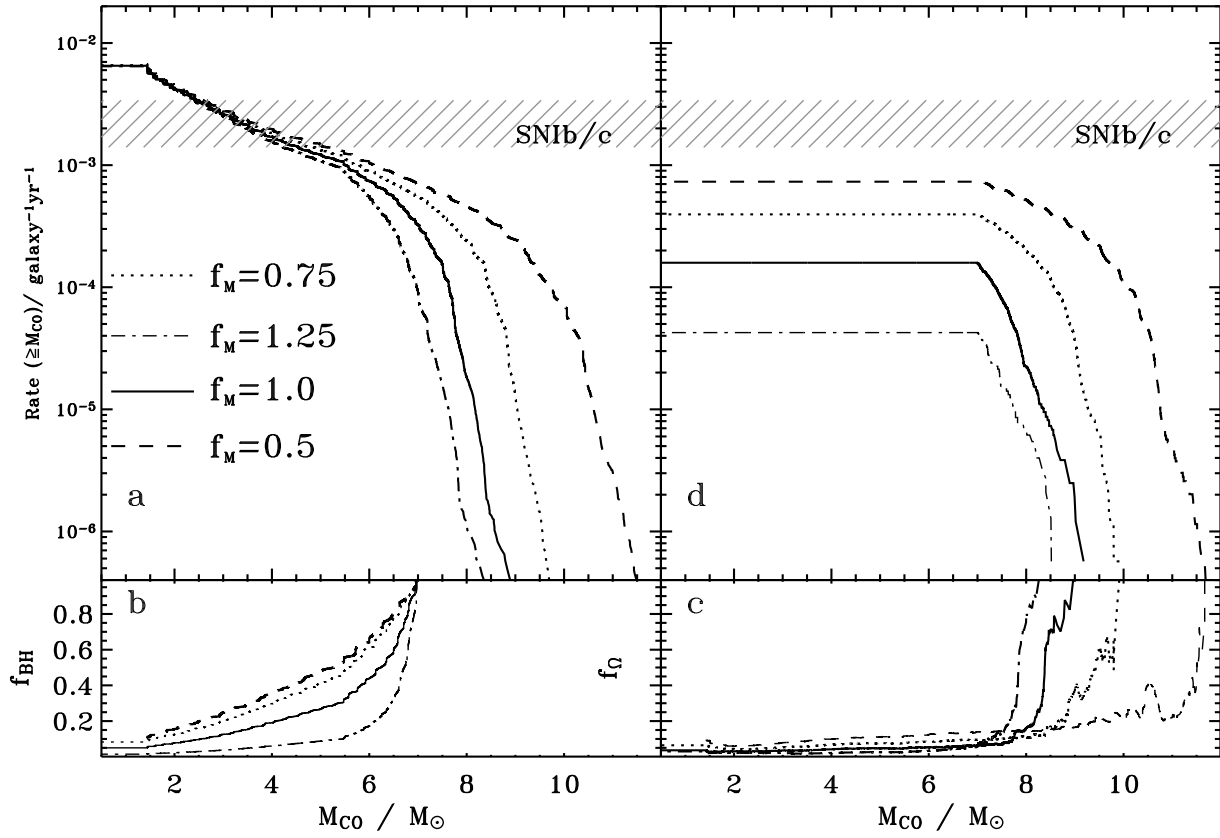


Figure 7. Similar to Fig. 2 for various f_M using an initial KTG-q distribution of binaries.

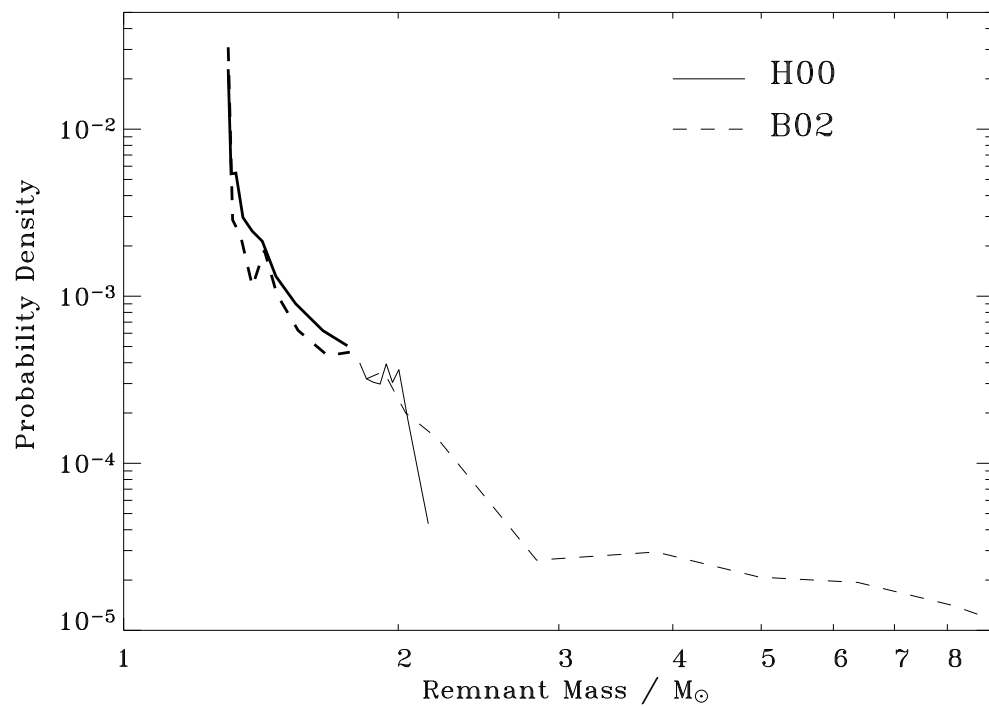


Figure 8. The probability distribution of final remnant masses for an initial KTG-q distribution of binaries and for two different prescriptions for NS (thick lines) and BH (thin lines) masses. See text for details.

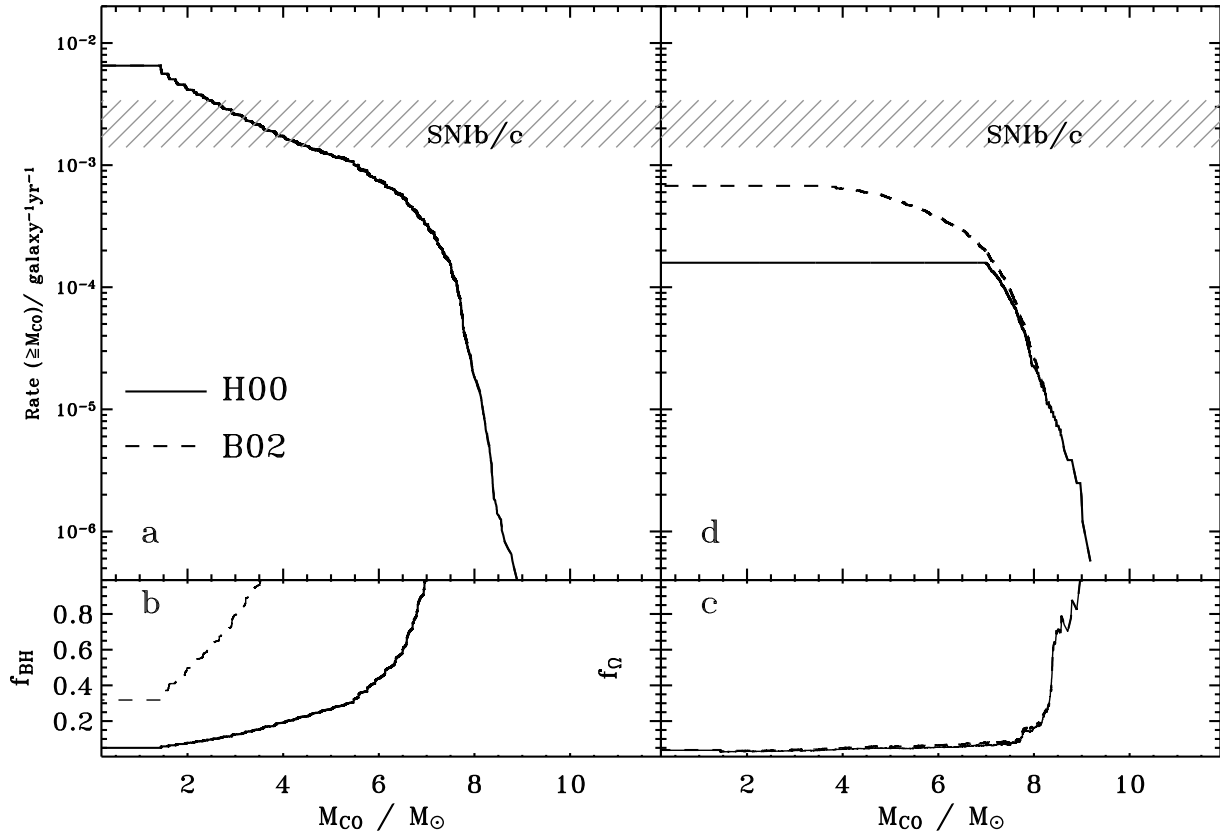


Figure 9. Similar to Fig. 2 but using the B02 prescription for NS and BH masses rather than the H00 formulae. An initial KTG-q distribution of binaries is adopted.

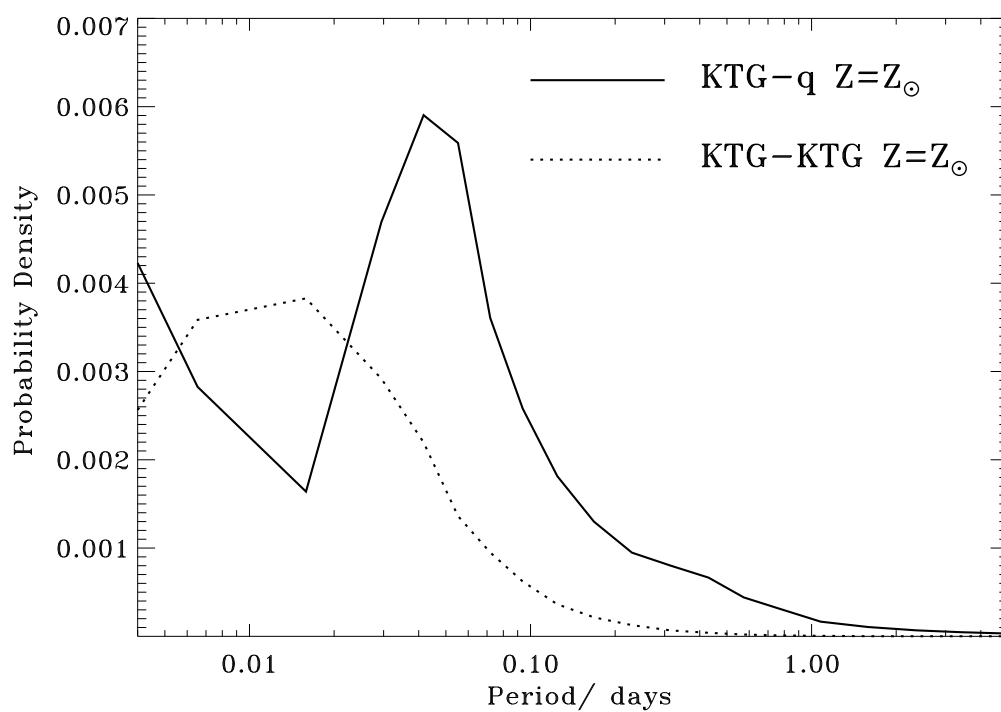


Figure 10. The probability distribution of binary period at the time when one of the stars explodes. The initial explosion then produces a BH and sufficient angular momentum to form a disc.

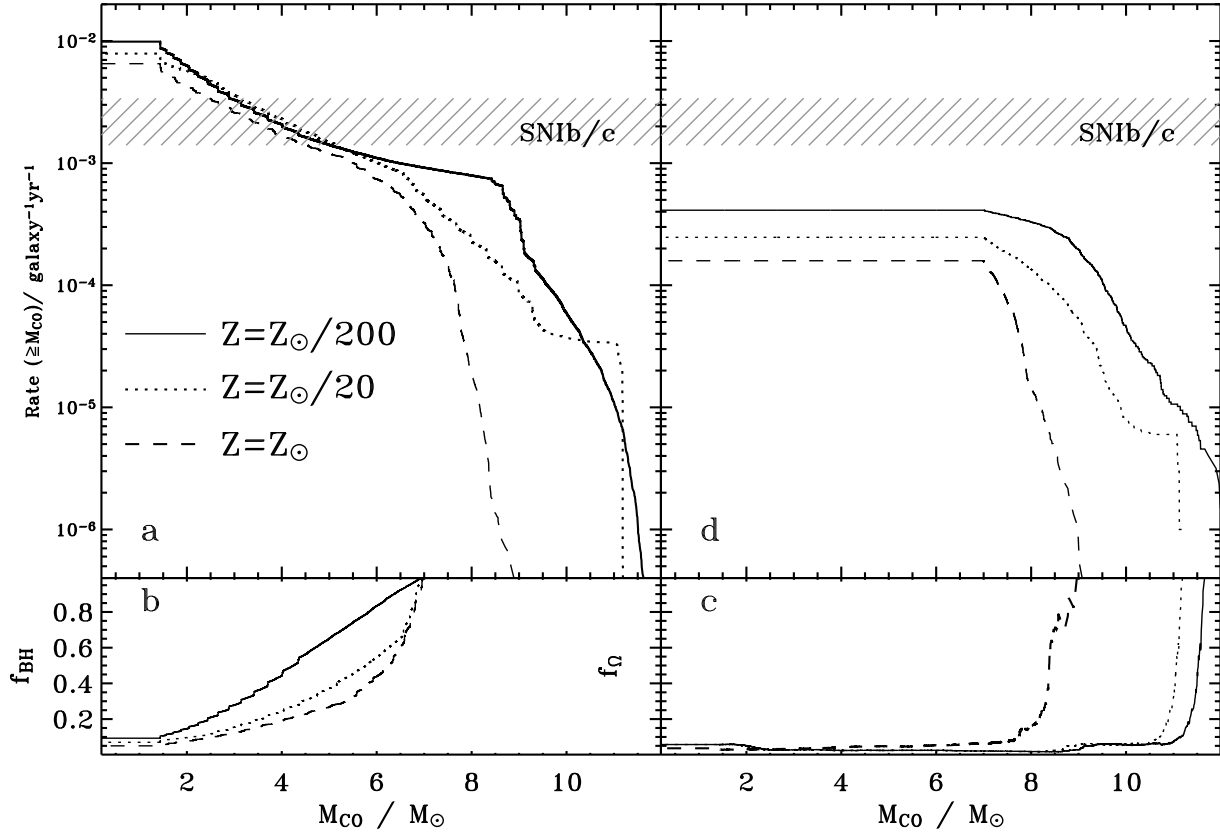


Figure 11. Similar to Fig. 2 for various Z using an initial KTG-q distribution of binaries.

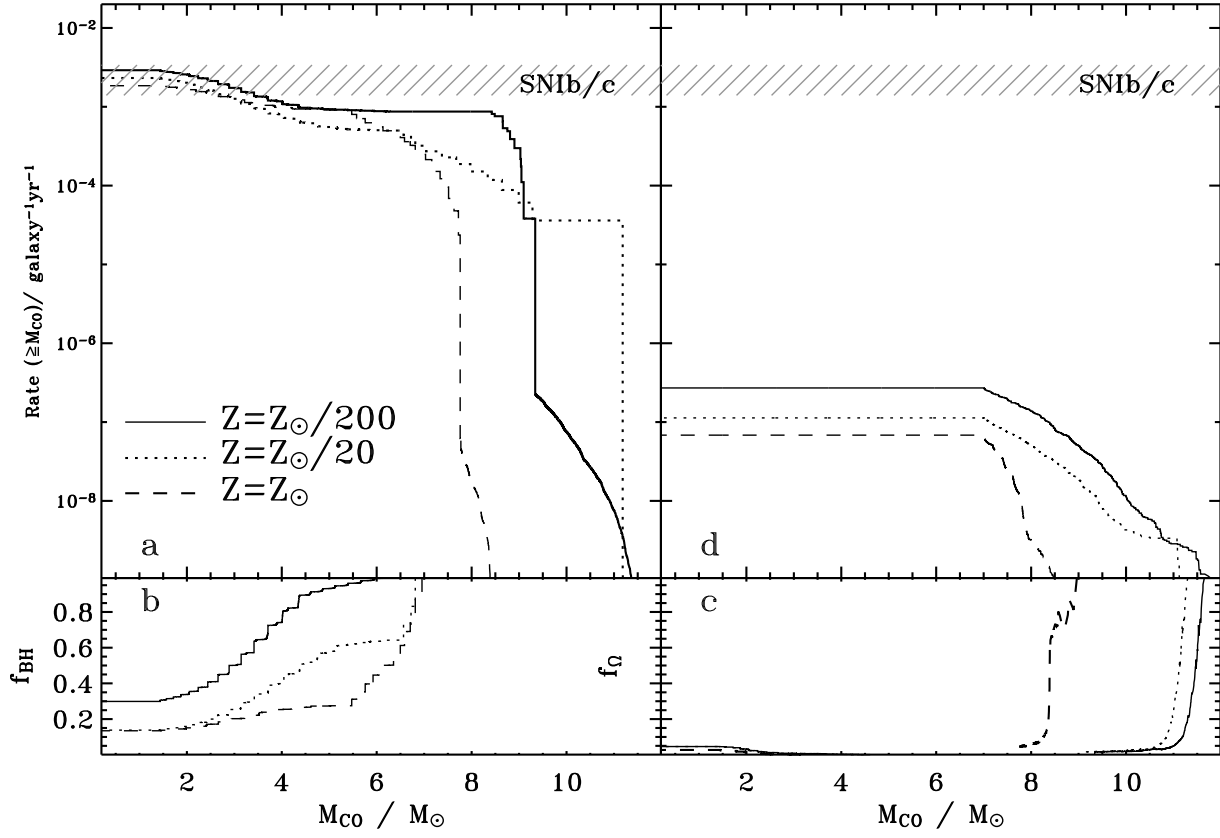


Figure 12. Similar to Fig. 11 but with an initial KTG-KTG distribution of binaries.

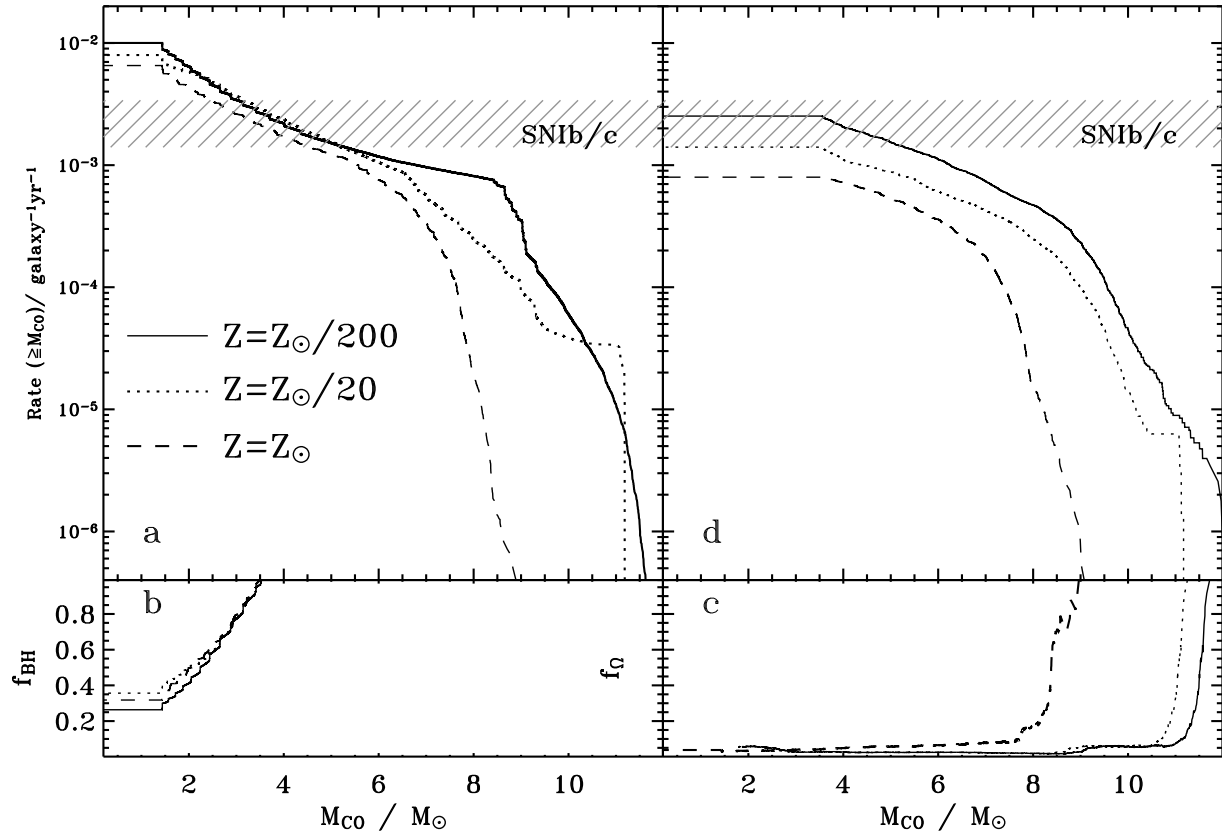


Figure 13. Similar to Fig. 11 but using the B02 prescription for NS and BH masses rather than the H00 formulae.

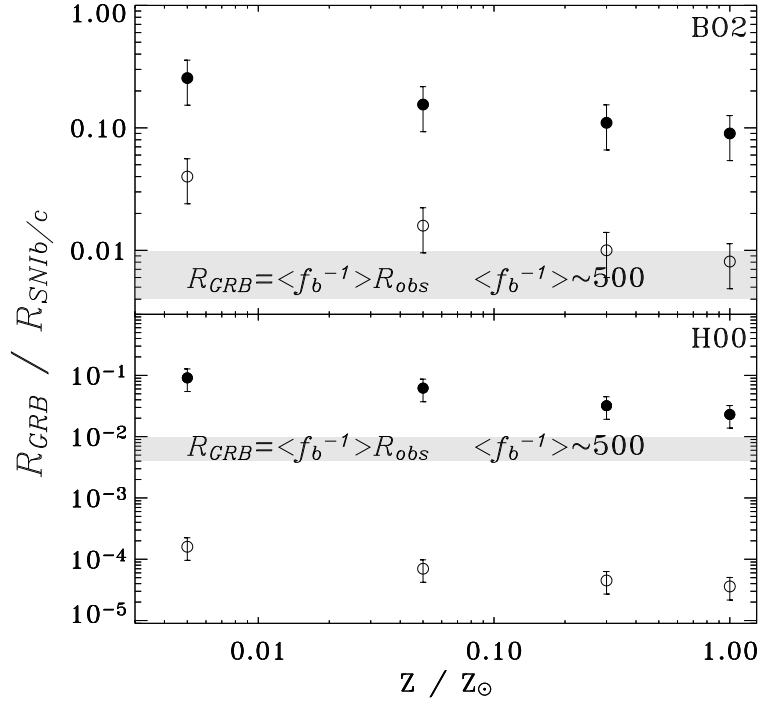


Figure 14. GRB formation rates as a function of metallicity for two different prescriptions for NS and BH masses. A GRB progenitor is thought to be a star that has both a massive enough core to form a BH and adequate rotation rate at the time of collapse to allow the formation of a centrifugally supported disc (see Section 3). The shaded region marks the 1σ width of the birth rate of GRBs as derived by Frail et al. (2001). The filled circles are KTG-q binary populations, the empty circles are binaries with an initial KTG-KTG distribution.